



SuperDove Geometric Quality Assessment Summary

Authors:

Alana G. Semple^{1,2}

Bin Tan^{1,2}

Guoqing (Gary) Lin²

*NASA CSDA Program Geometric
Subject Matter Experts*

¹ Science Systems and Applications Inc. (SSAI) Lanham, Maryland

² NASA Goddard Space Flight Center, Greenbelt, Maryland

Table of Contents

- 1. EXECUTIVE SUMMARY 1**
- 2. DETAILED VALIDATION – GEOMETRIC 2**
 - 2.1 Sensor Spatial Response (SSR) 2
 - 2.1.1 Method 2
 - 2.1.2 Results Compliance 3
 - 2.2 Absolute Positional Accuracy (APA) 3
 - 2.2.1 Method 3
 - 2.2.2 Results Compliance 4
 - 2.3 Band-to-Band Registration (BBR) 5
 - 2.3.1 Method 5
 - 2.3.2 Results Compliance 5
 - 2.4 Temporal Stability 6
 - 2.4.1 Method 6
 - 2.4.2 Results Compliance 6
- 3. REFERENCES..... 7**
- 4. APPENDIX 8**



1. EXECUTIVE SUMMARY

We have evaluated Planet’s SuperDove series spatial performance, relative geolocation accuracy over 25 globally distributed locations, band-to-band registration (BBR), and temporal stability at one USA city.

We constructed SuperDove’s sensor spatial response (SSR) for 5 of their sensors, each from a different launch. For the earliest four launches, we examined two scenes: one soon after launch and one 1+ years later. The average spatial response for all sensors and all bands examined (RGB) in the row direction for Relative Edge Response (RER) is 0.22 and in terms of Full Width Half Max (FWHM) is 3.28 pixels and in the column direction RER = 0.22, FWHM = 3.30 pixels. Modulation Transfer Function (MTF) at Nyquist frequency is 0.010 for all bands in the row direction, and 0.009 in the column direction.

SuperDove’s absolute geolocation accuracy (APA) varies by city when comparing with WorldView images as the reference image. Their self-consistencies (CE90-demean) are within 2 pixels. Overall accuracy by continent is:

Continent	# of Images	CE90 (m)	CE90-demean (m)
NA	56	7.21	3.39
SA	24	7.26	2.71
EU	25	25.98	4.31
AF	22	7.03	2.67
AUS	18	14.56	3.49
ASIA	30	11.44	6.67
Global	175	13.76	3.80

Band-to-Band Registration (BBR) for the SuperDove series after the archive was reprocessed is sub-pixel. See below chart for the radial offsets between every band and the red band.

Band vs. Red	# of Valid Matches	Mean(r_i) (m)	CE50(r_i) (m)	CE90(r_i) (m)
Costal Blue	79726	0.69	0.47	1.26
Blue	81598	0.52	0.34	1.01
Green I	94215	0.44	0.30	0.82
Green	109539	0.40	0.28	0.73
Yellow	125743	0.39	0.26	0.68
Red Edge	101528	0.50	0.31	0.93
NIR	41913	1.13	0.73	2.36

Temporal stability for one year was assessed at Albuquerque, NM. The temporal trend is steady over the year examined, and offsets vary from 0.00 m – 2.24 m in both the north-south and east-west directions.



2. DETAILED VALIDATION – GEOMETRIC

2.1 Sensor Spatial Response (SSR)

2.1.1 Method

Assessment of sensor spatial response is done with images over the Baotou, China Cal/Val location with a set of black and white squares slightly slanted with respect to the image grid direction [Baotou | EROS CalVal Center of Excellence (usgs.gov)]. The SuperDove series consists of many different aged sensors. There have been five launches of ‘Flocks’ in the SuperDove series, and we evaluate SSR for a single sensor in each of the four earlier Flocks from soon after launch and 1+ year later. The most recent Flock was launched in 2023, so only images soon after launch could be examined. We calculated SSR metrics for bands Red, Green, and Blue because other bands were too noisy for the method described here.

For each direction along row or along column, assessment starts with reading in 10 x 20 rows and columns across the black/white (B/W) transition (Fig 1a). A transition line location is estimated based on visual inspection of each image. Pixels are then transformed from bins to distance (Fig. 1b) from the transition line with the equation $d_p = d \cdot \cos(\Theta)$, where Θ is the angle between the line and horizontal/vertical, d is the horizontal/vertical distance from the pixel center to the transition line, and d_p is the perpendicular distance from pixel center to the transition line.

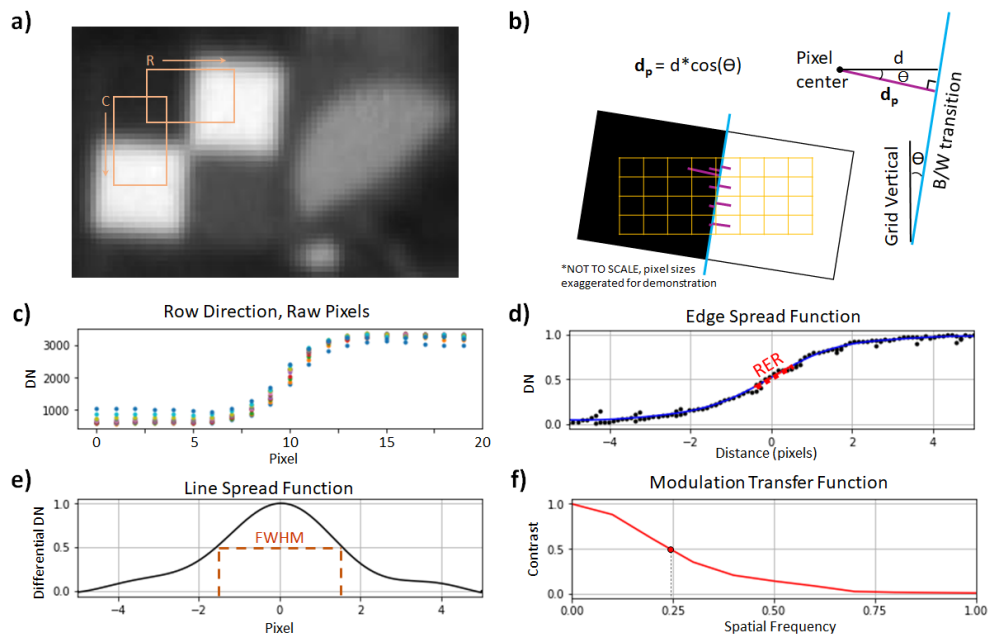


Figure 1. Visual demonstration of our SSR calculations. a) SuperDove blue band image (20220805_030006_84_2231) over Baotou, China site. Orange overlay squares indicate regions used in Edge Spread calculations in the row (R) and column (C) directions. b) Sub-pixel resolution is calculated based on pixel center distance (purple lines) from the black-to-white (B/W) color transition (blue line). Example demonstration is for the row direction. c) Raw pixels read in from box R in Fig.1a, colored by row. d) Sub pixel edge response constructed based on Fig.1b (black points) with a polynomial fit line (blue) for the Edge Spread Function (ESF). Region used in Relative Edge Response (RER) calculation is marked with a red dotted line, here it is 0.21. e) Line Spread function (LSF) is the derivative of ESF (Fig.1d). FWHM is shown in brown dashed lines, here it is 1.0. f) Modulation Transfer Function (MTF) plot showing Contrast vs Spatial Frequency.



3.22 pixels. f) Modulation Transfer Function (MTF) is the Fourier Transform of the LSF (Fig.1e). Here, the x axis is normalized by Nyquist Frequency = 1 cycle in 2 pixels. GRD is calculated based on the inverse of the frequency where $MTF = 0.5$ (red dot). Here, GRD is $1/.25 = 4.00$ pixels.

Once the values are transformed into distance from the B/W transition, a polynomial is fit to the line, creating an Edge Spread Function (ESF) (Fig. 1d). The slope of the central region of the ESF (from -0.5 – 0.5 pixels) gives the Relative Edge Response (RER). The derivative of the ESF is the Line Spread Function (LSF) (Fig. 1e) in the direction of interest. Full Width at Half Maximum (FWHM) is found from this LSF to represent the sensor’s effective footprint size. Finally, the Fourier transform of the LSF gives the Modulation Transfer Function (MTF) (Fig. 1f). Two more metrics for spatial response are found with the MTF curve, MTF value at Nyquist frequency and half wavelength where the MTF response reduces to half (we call this value Ground Resolved Distance (GRD)).

2.1.2 Results Compliance

SuperDove’s average spatial resolution expressed in RER is 0.22 in both directions and expressed in FWHM of LSF is 3.28 pixels in row direction and 3.30 pixels in column direction. Each band has a similar response. SSR improves with time as the sensors drop from their original launch orbit. The most recently launched sensor performs better than all sensors examined. See Appendix Table A2 for each sensor response evaluated.

2.2 Absolute Positional Accuracy (APA)

2.2.1 Method

Evaluation of SuperDove geolocation accuracy is a relative assessment with the panchromatic band of WorldView (WV) -2 and -3 images as the reference. WorldView imagery has a resolution of 0.3 m - 0.8 m and a CE90 of 5.4 m [DigitalGlobe Inc, 2016]. We orthorectify WV images with the 30 m SRTM DEM. SuperDove data is delivered orthorectified, so we do not orthorectify SuperDove data.

We have evaluated 25 locations of interest (Figure 2). Locations of interest for evaluation are either within cities or at airports. They all follow the criteria of at least 3 km² with minimal tree cover, low buildings, and no clouds. At this resolution, changing tree texture and building shadows will interfere with the matching algorithm. We would like to note that this is a best-case scenario evaluation done over locations with easy to match features. Many science teams will be working with remote locations that are harder to match and should expect worse geolocation accuracy than what we report here.

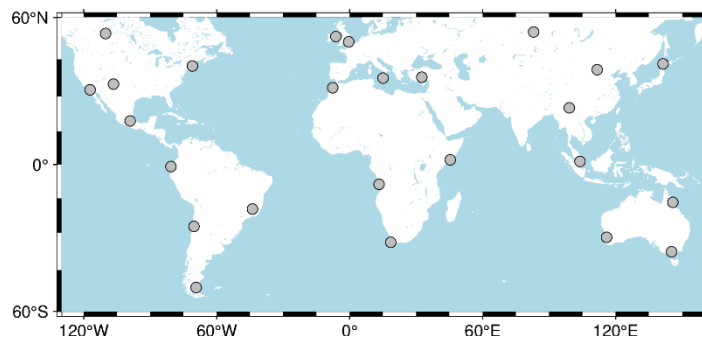


Figure 2. Global map of locations evaluated, marked with gray circles.



The assessment algorithm starts by determining the area of overlap between reference and target images. This overlapped region is then split into subset images of 250 m x 250 m chips. Each chip in the target image has a matching chip in the reference image based on the image's geolocation metadata. The algorithm then imposes offsets on the target chip of the pair and calculates the Pearson Cross Correlation (PCC) coefficient (a measurement of how well two images match). The offsets that give the best PCC are taken to be the geolocation offset between the chip pair. Quality of chip co-registration is then calculated with a Measurement Uncertainty (MU) equation [De Luccia et al. 2016] and used to filter out poor quality chip matches [Semple et al, 2023]

Where possible, we acquire 5 WV images over the area of interest and assess the WV images to find which images group. The most central image of the grouping is used as our main reference image when evaluating SuperDove's geolocation accuracy. This increases our confidence in the accuracy of the reference data. Some locations evaluated had either poor grouping, or we were only able to acquire 1 image of the area of interest, these locations are marked with an asterisk(*) in the full results table in the Appendix (Table A1).

Most metrics we calculate are standard metrics, except one we will introduce here, CE90-demean. CE90-demean is similar to the standard CE90 calculation but assumes there is no systematic bias between the SuperDove and reference images. CE90-demean measures the uncertainty of SuperDove's geometric calibration system. Figure 2 shows a visual demonstration of CE90 vs CE90-demean where the two values are different. In Figure 2, the largest contributor to the offset between SuperDove and WV images is likely due to offsets in their internal Ground Control Points (GCPs)/reference imagery.

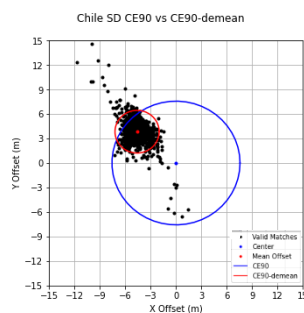


Figure 3. Chile's CE90 (blue circle) and CE90-demean (red circle) difference shows grouping of evaluated SuperDove offsets (black points) off-center from the reference WV image.

2.2.2 Results Compliance

SuperDove data is internally consistent, but when compared to WV imagery there are offsets that vary greatly by location.

We find that SuperDove's geolocation accuracy ranges from 3.20 m – 28.90 m offset for CE90 (relative to WV) but is only 1.99 m – 9.19 m offset when considering CE90-demean (essentially relative to itself). Figure 3 shows global offsets when considering CE90 (Fig 3 left) and CE90-demean (Fig. 3 right). Globally, SuperDove has a CE90 of 13.76 m, and a CE90-demean of 3.80 m. See the appendix for a table of all findings. Planet has been notified of these findings, and specially examined their Turkey data due to the large offsets we found there. Planet found that their data is self-consistent and well geolocated to their reference data (within 2 m). This is consistent with our CE90-demean results of the Turkey location.

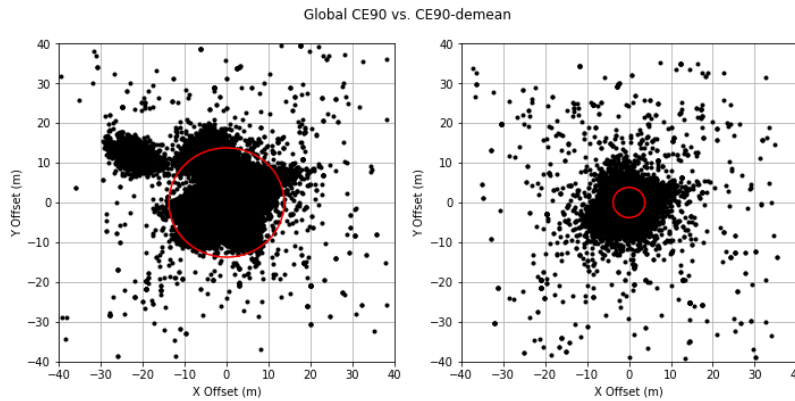


Figure 4. Plots of relative offsets for all SuperDove data. Left image plots CE90, right plots CE90-demean. Valid matches are plotted as black dots, and the CE90 circle as red circles.

2.3 Band-to-Band Registration (BBR)

2.3.1 Method

Band-to-band registration (BBR) is assessed with the image matching algorithm that is described above in the APA section. Each band of an image is assessed with its corresponding red band as the reference. We note that as the bands move farther from red (spectrally) the number of valid matches drops. The NIR band has less than half the number of valid matches that the Green Yellow and Red Edge bands have and performs the poorest (Table 1).

2.3.2 Results Compliance

The spectrally closer bands to red perform the best, and most bands are less than 1/3 of a pixel offset from the red band. NIR is the farthest offset at mean r_i in the x direction of 1.13 m. See Table 1 for the full list of BBR results. The radial offset of each valid chip match is r_i , where;

$$r_i = \sqrt{x_i^2 + y_i^2}$$

The east-west and north-south offsets of each valid chip match are x_i and y_i , respectively.

Table 1. BBR of all bands with Red band as reference.

Band vs. Red	# of Valid Matches	Mean(r_i) (m)	CE50(r_i) (m)	CE90(r_i) (m)
Costal Blue	79726	0.69	0.47	1.26
Blue	81598	0.52	0.34	1.01
Green I	94215	0.44	0.30	0.82
Green	109539	0.40	0.28	0.73
Yellow	125743	0.39	0.26	0.68
Red Edge	101528	0.50	0.31	0.93
NIR	41913	1.13	0.73	2.36



2.4 Temporal Stability

2.4.1 Method

Temporal stability is assessed with the image matching algorithm that is described above in section 1.2.1. Images at Albuquerque, NM are examined, with the earliest SuperDove image in the set used as the reference image. We acquired at least one SuperDove image per month for 1 year of temporal coverage. Including a few 1-day pairs, we obtained 14 images over this area.

2.4.2 Results Compliance

SuperDove is stable over the year of Albuquerque, NM data. The average offsets of each image (Fig. 5) vary from 0.03 m – 2.24 m in the east-west (EW) direction, and from 0.00 m – 2.23 m in the north-south (NS) directions.

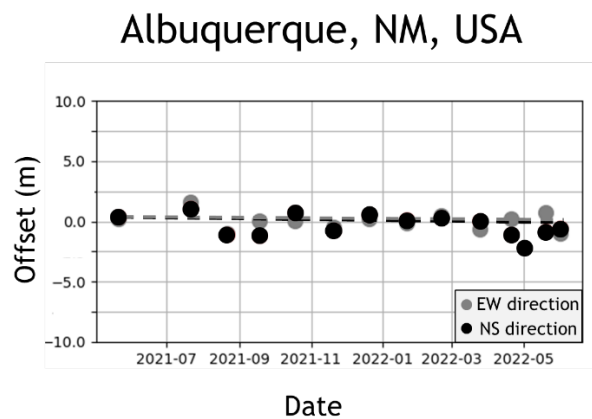


Figure 5. Time series stability plot for Albuquerque, NM. Mean offsets in the north-south (black) and east-west (gray) directions are plotted as dots. Trend lines are plotted as dashed lines in black for the north-south direction and gray for the east-west direction.



3. REFERENCES

De Luccia, F. J., Houchin, S., Porter, B. C., Graybill, J., Haas, E., Johnson, P. D., Isaacson, P. J., and Reth, A. D. (2016), "Image navigation and registration performance assessment tool set for the GOES-R Advanced Baseline Imager and Geostationary Lightning Mapper", Proc. SPIE 9881, Earth Observing Missions and Sensors: Development, Implementation, and Characterization IV, 988119 (2 May 2016); doi: 10.1117/12.2229059.

DigitalGlobe Inc. (2016), "Accuracy of worldview products". [White Paper pdf](#). Last accessed 15 June 2023.

Semple, A., B. Tan, and G. Lin. (2023), "[Automation of Geometric Accuracy Assessment Algorithm](#)", JACIE 2023 Workshop.

USGS [Spatial Sites Catalog | EROS CalVal Center of Excellence \(usgs.gov\)](#). Last accessed 15 June 2023.



4. APPENDIX

Table A1. Relative geolocation accuracy assessment results. Asterisk (*) by the city name indicates locations where either only 1 WV image was obtained or the WV images did not group, leading to less certainty in the reference image's accuracy.

A City Within:	# of SD Images	# of Valid Matches	X Offset (m)	Y Offset (m)	X StdDev (m)	Y StdDev (m)	X RMSE (m)	Y RMSE (m)	CE90 (m)	CE90-demean (m)
Massachusetts	14	3683	1.25	-6.07	3.03	3.75	3.28	7.13	4.34	2.02
California	11	2257	-2.17	0.32	1.70	1.83	2.76	1.86	3.53	2.34
New Mexico	20	6072	-0.35	-0.32	1.86	1.45	1.89	1.48	3.20	3.23
Canada*	6	517	1.38	2.01	1.99	3.16	2.42	3.74	6.04	5.17
Mexico	5	4361	2.04	0.98	1.51	1.41	2.54	1.72	4.45	3.06
Ecuador	6	408	-5.57	-7.59	1.63	2.25	5.81	7.92	11.28	2.58
Brazil	6	6848	-0.94	3.29	0.95	1.63	1.34	3.67	5.14	2.56
Chile	5	1023	-4.60	3.83	1.23	1.59	4.76	4.15	7.57	2.61
Argentina	7	1851	-2.52	-5.37	1.68	1.54	3.03	5.58	7.85	3.08
England	6	2727	-3.69	12.79	1.86	2.83	4.13	13.10	16.62	4.62
Ireland	5	2668	-1.05	10.32	1.43	1.47	1.77	10.42	12.27	3.01
Sicily	5	2182	-5.76	10.38	4.32	5.10	7.20	11.57	15.74	5.03
Turkey*	9	2901	-21.98	12.19	2.37	1.87	22.11	12.33	28.09	4.54
Morocco	5	1182	4.30	2.04	4.96	4.16	6.56	4.63	6.98	2.71
Angola	6	4292	3.77	0.38	0.76	1.53	3.85	1.58	5.05	2.64
Somalia	5	5244	-1.17	0.98	1.27	1.16	1.73	1.52	3.33	2.61
South Africa	6	4597	-6.23	0.06	1.64	1.18	6.44	1.18	8.22	2.73
Cairns	6	2758	1.72	-0.27	2.98	3.71	3.44	3.72	5.99	4.96
Melbourne	6	2485	-10.06	9.83	0.98	1.65	10.10	9.97	15.22	1.99
Perth	6	3387	-7.63	-7.48	1.81	1.55	7.84	7.64	13.22	3.64
Baoshan	7	2920	-0.88	-1.00	2.46	2.92	2.61	3.09	4.87	4.35
Hohhot	5	1569	-9.37	-1.39	1.98	1.56	9.57	2.09	11.72	3.21
Japan	6	4434	5.00	-7.20	1.16	1.82	5.13	7.43	11.11	3.26
Russia*	6	1463	4.64	3.27	1.89	1.79	5.01	3.72	7.34	2.47
Singapore	6	4159	5.50	4.42	6.36	6.54	8.41	7.89	14.32	9.19
NA	56	16890	0.43	-1.08	2.51	3.52	2.55	3.68	7.21	3.39
SA	24	10130	-1.79	1.32	1.83	4.16	2.56	4.37	7.26	2.71
EU	25	10478	-8.52	11.49	8.88	3.19	12.30	11.93	25.98	4.31
AF	22	15315	-0.88	0.62	4.49	1.78	4.58	1.89	7.03	2.67
AUS	18	8630	-5.34	-0.19	5.36	7.48	7.57	7.48	14.56	3.49
Asia	30	14545	2.37	-0.95	6.03	6.12	6.48	6.20	11.44	6.67
Global	175	75988	-1.65	1.44	6.26	6.12	6.48	6.29	13.76	3.80

Table A2. Sensor spatial response for 5 sensors, one from each SD 'Flock' launch. For the earlier four Flocks, we examine two images for that sensor, an image soon after launch and one as close to current (06/2023) as possible, depending on availability.

[Mission/Instrument] Quality Assessment Summary

Issue: 1.0



Sensor (image date)	Pixel Size (m)	Band	RER				RER			
			FWHM (pix)	GRD (pix)	MTF @ny	FWHM (pix)	GRD (pix)	MTF @ny		
			Row Direction				Column Direction			
24b0 (06/23) Y	3.0	R	0.29	2.57	4.00	0.004	0.29	2.59	4.10	0.004
		G	0.30	2.67	3.90	0.049	0.30	2.70	4.00	0.031
		B	0.30	2.69	3.75	0.040	0.30	2.71	3.75	0.028
2478 (03/22) X	3.0	R	0.23	3.14	4.20	0.007	0.23	3.20	4.20	0.008
		G	0.23	3.10	4.20	0.008	0.23	3.11	4.00	0.010
		B	0.24	3.00	4.00	0.007	0.24	3.05	4.00	0.009
2478 (03/23) X	3.0	R	0.24	3.06	4.20	0.011	0.23	3.10	4.20	0.010
		G	0.22	3.24	4.20	0.011	0.22	3.25	4.20	0.011
		B	0.24	2.93	4.00	0.006	0.24	3.02	4.00	0.005
2420 (03/21) S	3.0	R	0.22	3.21	4.20	0.007	0.22	3.25	4.20	0.007
		G	0.20	3.53	4.33	0.008	0.20	3.55	4.33	0.007
		B	0.23	3.21	4.10	0.010	0.22	3.23	4.20	0.009
2420 (03/23) S	3.0	R	0.24	2.84	4.20	0.012	0.24	2.85	4.33	0.010
		G	0.20	3.55	4.33	0.010	0.20	3.57	4.33	0.008
		B	0.24	2.93	4.20	0.013	0.24	2.93	4.33	0.009
2254 (10/20) V	3.0	R	0.14	4.21	4.50	0.002	0.14	4.21	4.50	0.005
		G	0.13	4.20	4.50	0.006	0.14	4.21	4.50	0.006
		B	0.13	4.15	4.50	0.007	0.13	4.17	4.50	0.010
2254 (10/22) V	3.0	R	0.20	3.33	4.20	0.009	0.20	3.36	4.20	0.009
		G	0.21	3.30	4.20	0.012	0.21	3.32	4.20	0.009
		B	0.21	3.31	4.10	0.008	0.21	3.32	4.10	0.010
2231 (09/20) P	3.0	R	0.20	3.87	4.00	0.010	0.19	3.90	4.00	0.009
		G	0.20	3.60	4.00	0.008	0.20	3.61	4.10	0.008
		B	0.20	3.86	4.00	0.008	0.20	3.88	4.00	0.002
2231 (08/22) P	3.0	R	0.22	3.19	4.10	0.005	0.22	3.19	4.10	0.006
		G	0.23	3.14	4.00	0.004	0.23	3.15	4.00	0.005
		B	0.23	3.16	4.00	0.007	0.23	3.16	4.00	0.007
Total (near Launch)	3.0	R	0.22	3.40	4.18	0.006	0.21	3.43	4.20	0.007
		G	0.21	3.42	4.19	0.016	0.21	3.44	4.19	0.012
		B	0.22	3.38	4.07	0.014	0.22	3.41	4.09	0.012
Total (After 1+ Years)	3.0	R	0.23	3.11	4.18	0.009	0.22	3.13	4.21	0.009
		G	0.22	3.31	4.18	0.009	0.22	3.32	4.18	0.008
		B	0.23	3.08	4.08	0.009	0.23	3.11	4.11	0.008